

INVESTIGATION OF THE DISINTEGRATION OF TA<sup>182</sup>

by

ROBERT JOSEPH KLOTZ

A. B., Kansas State Teachers College, Emporia, 1952

---

A THESIS

submitted in partial fulfillment of the

requirements for the degree

MASTER OF SCIENCE

Department of Physics

KANSAS STATE COLLEGE  
OF AGRICULTURE AND APPLIED SCIENCE

1954

LD  
2668  
T4  
1954  
K55

11  
125

C.2  
Documents

# TABLE OF CONTENTS

INTRODUCTION . . . . .	1
General Theory of the Beta Ray Spectrometer . . . . .	4
Statement of Purpose . . . . .	6
EXPERIMENTAL APPARATUS . . . . .	6
Low Field Magnet and Associated Cameras . . . . .	7
The Magnet . . . . .	7
The Photographic Cameras . . . . .	8
The Variable Radius Spectrometer . . . . .	13
High Field Magnet and Camera . . . . .	14
The Radioactive Sources . . . . .	16
CHARACTERISTICS OF A VARIABLE RADIUS BETA RAY SPECTROMETER . . . . .	17
Experimental Methods . . . . .	17
Discussion of Results . . . . .	21
INVESTIGATION OF TA <sup>182</sup> . . . . .	26
Experimental Methods . . . . .	26
Discussion of Results . . . . .	31
ACKNOWLEDGMENT . . . . .	34
BIBLIOGRAPHY . . . . .	35

## INTRODUCTION

Extensive research is necessary before a complete theory of the nucleus of the atom can be obtained. One line of research has been through the study of disintegration schemes of radionuclides.<sup>1</sup> Although much useful information of this type has already been obtained, much more remains to be done, particularly for the even-even isotopes.<sup>2</sup> This report deals with the disintegration scheme of tungsten 182, one of a family of even-even isotopes under investigation in a more extensive research project at Kansas State College.

A radionuclide, not found in nature, is obtained by bombardment of a stable nuclide by an energetic particle or gamma ray that is able to enter and remain in the nucleus, thus transforming the stable nuclide to a radionuclide. The radionuclides investigated in this study were obtained by pile neutron bombardment at the Argonne National Laboratory.

Radionuclides decay by any of the following processes: alpha emission, beta emission, and gamma emission. Beta emission comprises the following types: negatron emission ( $\beta^-$ ), in which a negatron is emitted by the nucleus; positron emission ( $\beta^+$ ), in which a positron is emitted by the nucleus, and K-capture (K), in which an orbital electron is captured by the nucleus. Combinations of these three basic processes are also observed upon occasion. A radionuclide after negatron emission changes to

---

<sup>1</sup> A radionuclide is a radioactive atom.

<sup>2</sup> Even-even isotopes have even mass numbers and even atomic numbers.

a new nuclide whose atomic number is increased by one. In the other basic beta processes the atomic number decreases by one. Following these beta processes there are usually found several monoenergetic gamma rays and conversion electrons, which are characteristic of the energies of the transitions between levels, as the nuclide goes to the ground state. A diagram indicating the energy levels and possible transitions is called a decay scheme. In the radionuclides studied here, only  $\beta^-$  emission and gamma emission (with the associated conversion electrons) are important.

Unlike other nuclear disintegration processes, the electrons taking part in  $\beta^\pm$  processes are accompanied by neutrino emission. Since the neutrinos also carry away energy, the electrons in such processes are not monoenergetic, but have a continuous distribution in energy whose maximum value has the transition energy value. If the maximum energies of the beta particles and relative intensities are known then it is possible to determine the newly formed nuclides' intermediate energy states as well as their populations, thus greatly facilitating the determination of the decay scheme. The beta particle energies vary from zero to the maximum (or transition value); therefore it is usually difficult to determine the maximum energy accurately, except by the well known Fermi-Kurie method of analysis (Wu, 21). This method of analysis is particularly advantageous when more than one spectrum is present.

As mentioned earlier, it is usually observed that both gamma rays and conversion electrons are emitted as the nuclide decays to its ground state. The conversion electron is the result of a process called internal conversion. This process occurs when a bound electron perturbs the excited nucleus inducing a transition to a lower energy state, the energy

being transferred to the electron. For a transition between two levels of a nuclide, there is a finite probability that the energy will be emitted either as a gamma ray or as a conversion electron. The ratio of the probability for a converted electron to that of an unconverted gamma ray (called the conversion coefficient) is determined by the multipole order and type, as well as the transition energy. Thus knowledge of conversion coefficients aids in the determination of the spins for the energy levels associated with the transition. The resulting energy imparted to the conversion electron ( $E_e$ ) is the transition energy ( $E_\gamma$ ) minus the binding energy (B.E.) of the orbit vacated by the electron.

$$(1) \quad E_e = E_\gamma - \text{B.E.}$$

Conversion electrons originate from the innermost electron shells. The ratio of the conversion coefficients for the various orbital shells are again determined by the angular momentum change and the energy. Thus measurements of conversion coefficient ratios furnish additional information for the construction of the energy level scheme.

Aside from information about angular momenta, equation (1) shows that the transition energy between two states,  $E_\gamma$  can be determined by measurement of the energy of the converted electron, since binding energies are now accurately known from other sources (Hill, et al., 12).

In many cases, conversion is such an improbable process, that energy measurements based upon conversion electron energies are relatively inaccurate. In these cases, it is sometimes convenient to employ a photoelectric radiator. Here, the unconverted gamma radiation is allowed to fall upon a secondary radiator (frequently lead, for example). The resulting

energy imparted to the photoelectron ( $E_e$ ) is equal to the energy of the gamma ray ( $E_\gamma$ ) minus the binding energy ( $B.E.$ )<sub>R</sub> of the electron ejected from the radiator.

$$(2) \quad E_e = E_\gamma - (B.E.)_R$$

The photoelectrons originate, as with internally converted electrons, more abundantly from the inner electron shells.

The processes described above all point out the advantages obtained from a knowledge of both energies and intensities of the electrons associated with nuclear disintegration. Beta-ray spectrometers and spectrographs are instruments whose functions are to determine these quantities. The following section takes up the theory of these instruments, while later sections describe the design and application of instruments employed in this research.

#### General Theory of the Beta Ray Spectrometer

Basically, the beta ray spectrometer serves to measure the momentum of electrons. Since energies are of the most interest the following derivation leads to the expression for energy in terms of momentum.

An electron of charge ( $e$ ), with momentum ( $P$ ), projected perpendicular to a magnetic field ( $B$ ) moves in a circular path of radius ( $\rho$ ). The force acting on the electron is directed toward the center of this circular path. The following equation holds relativistically

$$(3) \quad Bev = \frac{mv^2}{\rho}$$

where ( $m$ ) is the relativistic mass of the electron. In terms of the momentum ( $P$ ) equation (3) becomes

$$(4) \quad P = mv = E\rho e$$

Expressing the relativistic mass ( $m$ ) in terms of the rest mass ( $m_0$ )

$$(5) \quad m = m_0 \left[ 1 - \left( \frac{v}{c} \right)^2 \right]^{-\frac{1}{2}}$$

where ( $c$ ) is the velocity of light. The relativistic kinetic energy ( $E$ ) is given by

$$(6) \quad E = (m - m_0)c^2$$

Substituting equation (5) into equation (6) the following relationship is obtained:

$$(7) \quad E = m_0 c^2 \left\{ \left[ 1 - \left( \frac{v}{c} \right)^2 \right]^{-\frac{1}{2}} - 1 \right\}$$

Eliminating ( $v$ ) between equation (7) and (4) the following equations relating  $E\rho$  and  $E$  are obtained:

$$(8) \quad E\rho = \left( \frac{1}{ce} \right) \left[ E^2 + 2m_0 c^2 E \right]^{\frac{1}{2}} = \frac{P}{e}$$

$$(9) \quad E = \left[ (m_0 c^2)^2 + (E\rho ce)^2 \right]^{\frac{1}{2}} - m_0 c^2$$

In terms of recent physical constants, as summarized by Diamond and Cohen (8), equation (9) may be reduced to

$$(10) \quad E = \left[ g^2 + d (E\rho)^2 \right]^{\frac{1}{2}} - g$$

where:  $g = 0.5108 \text{ mev.}$

$$d = 8.9867 \times 10^{-8} \text{ mev}^2/\text{gauss}^2\text{cm}^2$$



It is seen from equation (10), that knowledge of the field intensity ( $B$ ) and the trajectory radius ( $\rho$ ) lead directly to the energy of the electron ( $E$ ).

#### Statement of Purpose

As implied by equation (10), beta ray spectrometers are instruments which utilize magnetic fields and trajectory defining slits to allow separation of electrons according to their energies. Several types of spectrometers are currently in use. One type, called the variable field spectrometer, uses a fixed trajectory radius with a variable field. Others, hereafter called variable radius spectrometers, employ fixed fields and allow focusing for variable radii. It was one of the purposes of this work to demonstrate the applicability of an instrument of this type to quantitative measurements, not only of electron energy values, but of intensities as well.

The variable radius spectrometer, along with several other instruments to be described later have been applied with some success to the analysis of the decay components of the radionuclide,  $Ta^{182}$ .

#### EXPERIMENTAL APPARATUS

Fixed field  $180^\circ$  focusing type beta ray spectrometers and spectrographs were employed throughout. Two different magnets with their associated cameras were available with each component having its specific



advantages. For quantitative intensity studies a camera with a geiger tube detector (hereafter referred to as a spectrometer) was employed. Conversion electron energies were obtained with a camera using photographic film for the detector. These instruments are later referred to as spectrographs.

A description of these instruments, as well as details such as development of film and preparation of radioactive sources, are given in following sections.

#### Low Field Magnet and Associated Cameras

The Magnet. The magnet, as seen in Plate I, Fig. 1, was constructed with soft iron circular pole faces, 16 inches in diameter. The yoke likewise was constructed of soft iron having a rectangular cross-sectional area of 64 square inches. The air gap could be adjusted but was fixed at 3 inches during this investigation. Permanent fields were secured by the inclusion of cylinders of Alnico III, 1 inch in diameter and 3 inches in height, placed between both pole pieces and the yoke in such a way that the magnetic flux passed from the pole pieces through the Alnico to the yoke. Excitation currents up to 50 amperes, supplied by two parallel D. C. generators, was conducted through two coils having approximately 310 turns of No. 6 copper wire per coil.

Magnetic fields up to 600 gauss between the pole pieces could be obtained with the larger excitation currents. The Alnico cylinders were spaced close together near the perimeter of the pole pieces to compensate

for the fringing flux, thus allowing reasonably uniform fields over the central 12 inch diameter region between the pole faces.

An essential feature of the magnet was its stability. Upon establishing a new field, after 24 hours no measurable shifts in magnetic field values were observed. Evidence for this stability was based upon the appearance of sharp conversion lines<sup>1</sup> in spectrograms having long exposure times and also by comparison of similar spectrograms taken at different times after establishing the field.

The Photographic Cameras. A pair of cameras of the same size and design was used in obtaining photographic data in the low field magnet. The cameras were so constructed that both could be employed in the magnet at the same time, thus doubling the output of the spectrograph. These cameras have been discussed in a thesis by Kruse (14), except for an alteration in the radioactive source holder. The holders were modified so that the same source could be used in all cameras employed in this research. The modified source holder and source frame can be seen on Plate II, Fig. 2.

Kodak No-Screen X-ray film and DK-50 developer were used exclusively. A constant temperature bath set the developing time at 5 minutes and the fixing time at 10-15 minutes. Films were washed in running cold water, immersed in Even-Flo, and allowed to dry at room temperatures under a slight tension to prevent warping.

---

<sup>1</sup> Monoenergetic electron groups focus roughly as lines parallel to the magnetic field. The words 'conversion line' and 'conversion electron group' have therefore become synonymous in the sense used above.

#### EXPLANATION OF PLATE I

- Fig. 1. Photograph of the spectrometer including the magnet, the variable radius spectrometer with the camera in operating position, the scaler and the filling system. The constant temperature bath for continuous ethyl alcohol supply is shown on the left side of the glass filling system panel.
- Fig. 2. A photograph of the interior of the variable radius spectrometer camera showing lead shielding between radioactive source and geiger tube. Control knob outside camera served to move the geiger tube along the threaded spindle.
- Fig. 3. Photograph of low field photographic camera showing the source frame attached to the source holder.

## PLATE I



Fig. 1

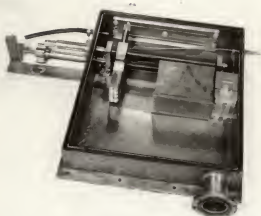


Fig. 2

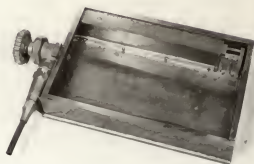


Fig. 3

EXPLANATION OF PLATE II

Fig. 1. Photograph of the high field photographic camera with a photographic film inserted on the focal plane.

Fig. 2. Photograph of the rear view of the source assembly. Shown is the radioactive source (the dark ribbon) attached to the source frame which is in turn rigidly held to the source holder by a set screw.

## PLATE II



Fig. 1

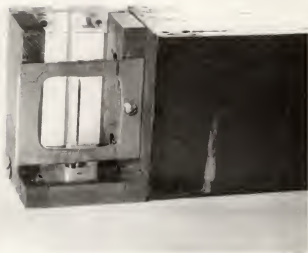


Fig. 2

The Variable Radius Spectrometer. The spectrometer camera was constructed of 3/8 inch brass plate with a removable top lid. A large vacuum port was flange-connected to a rigid coupling attached to the stack of a diffusion pump. This made it possible to reduce the pressure rather quickly to about 5 microns of mercury where it was maintained during operation. The detector, a rectangular geiger tube, was designed to move along a threaded spindle in such a way that the geiger tube window opened upon the focal plane.<sup>1</sup> The geiger tube motion was controlled by a turning knob, located on the exterior of the camera, attached to the spindle through a conventional O-ring vacuum seal. A Veeder-Root counter attached to the spindle recorded the position of the tube. The geiger tube was filled through a tygon tube connected to an exterior filling system. The interior of the camera, with internal lead shielding, is shown on Plate I, Fig. 2.

The flexible tygon filling couplings presented some difficulties. It was found that this tubing (as well as other flexible couplings tried) absorbed organic quenching gases from the system. This caused the geiger tube threshold voltage to decrease, giving rise to erratic operating conditions. After considerable research a method was found for maintaining steady geiger tube operating conditions, based upon a continuous replacement of absorbed quenching agent. A source of ethyl alcohol, the quenching agent employed, maintained at 0° Centigrade and opened to the geiger

---

1 In the fixed field 180° type spectrometer, monoenergetic electrons are brought to an approximate focus on a plane running parallel to the field and through the defining slits, this plane is called the focal plane.



tube system furnished a continuous source of alcohol at a good working pressure. To maintain the alcohol temperature at 0° Centigrade, the tube of alcohol was immersed in an ice and water bath. The vapor pressure of ethyl alcohol of 0° Centigrade, and thus the pressure furnished to the system, was about 1.20 centimeters of mercury. A 10 percent ethyl alcohol and 90 percent argon mixture, at around 12 centimeters total pressure, gave good geiger tube operating characteristics. It was found best to premix the alcohol and argon, before admitting the mixture to the geiger tube. Two to three hours after admitting the mixture to the geiger tube equilibrium was obtained between absorption and replacement of alcohol in the system, thus resulting in very stable operating conditions.

A typical plateau of the geiger tube is shown in Fig. 1. This plateau exhibits a 9.0 percent rise per 100 volts over a 160 volt range.

A Nuclear Corporation scaler supplied the high voltage for the geiger tube anode and registered the events detected by the tube.

The spectrometer camera, filling system, low field magnet, and scaler are all shown in Plate I, Fig. 1 in operating position.

#### High Field Magnet and Camera

The low field magnet previously described, was capable of accurately focusing electrons with energies up to 1.6 mev. This limit was set by the maximum obtainable field of 600 gauss and a maximum focusing radius of around 11 centimeters. To study higher energy electrons, the magnet,

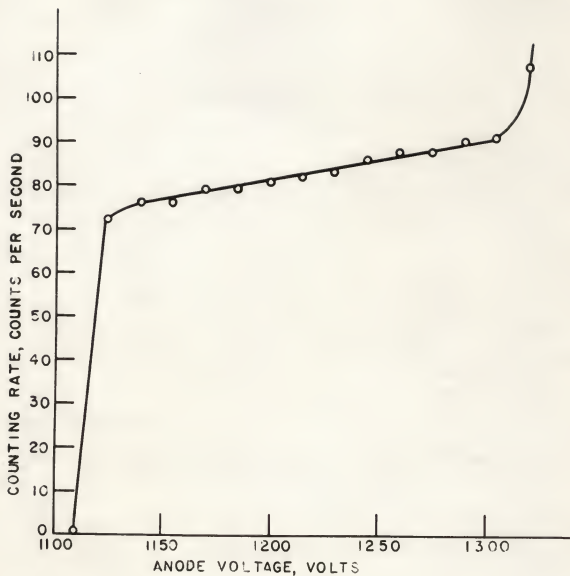


Fig. 1. Typical geiger tube plateau exhibiting a 9.0 percent rise per 100 volts.

previously described by Mellor (16), was altered by decreasing the pole gap to  $1 \frac{3}{4}$  inches. Fields up to 800 gaussess were then obtained. Larger focusing radii were also possible, since the fringing flux was decreased, thus allowing a larger portion of the pole face area to be utilized. With the magnet, and its associated camera, electron energies in excess of 3 mev could be studied.

A second feature of the high field camera was the increase in intensity brought about by focusing conversion groups at smaller radii. The explanation of this feature is given subsequently.

A photographic camera of reduced height, and capable of focusing conversion groups of larger radii was designed much like that described by Kruse (14). To keep the camera interior height as large as possible, thus allowing the largest possible film height,  $1 \frac{1}{4}$  inch brass plates were used for the top and bottom of the camera. To reduce the fogging of the film from photoelectric and Compton electrons which formed at the lead shielding surface, a  $1 \frac{1}{2}$  inch lucite piece was glued to the photographic film plane. The interior of the camera, with film and radioactive source in place, is shown in Plate II, fig. 1.

#### The Radioactive Sources

The radioactive isotopes used in this investigation were  $\text{Ir}^{192}$  and  $\text{Ta}^{182}$ .

The sources were prepared by sticking the radioactive materials,

in the form of powder, on the adhesive side of narrow pieces of "Scotch" tape. These tapes, in turn, were mounted on aluminum source frames. One of these assemblies, usually referred to more simply as a source, is shown on Plate II, Fig. 2, attached to the camera source holder.

#### CHARACTERISTICS OF A VARIABLE RADIUS BETA RAY SPECTROMETER

The fixed field  $180^\circ$  focusing variable radius spectrometer may be used to determine quantitative intensity data only when the characteristics ( $h$ ) of the spectrometer have been determined. One important characteristic is the variation of the intensity with the change in solid angle subtended from the source by a detector located at different positions on the focal plane. Theoretical determination of this factor was not feasible because of scattering and absorption of particles incident on the sides of the detector slits. Consequently, a method of obtaining this, as well as other characteristics, experimentally will be presented.

#### Experimental Methods

The solid angle factor, designated as the  $\rho$ -factor throughout the remaining text, was determined for the variable radius spectrometer with the following dimensions held fixed during the entire experimental proceedings.

Distance from source to focal plane	2.0 cm
Source width	1.0 mm

Source height	3.3 cm
Slit width	6.0 mm
Slit height	3.3 cm
Detector slit width	1.5 mm
Detector slit height	2.5 mm

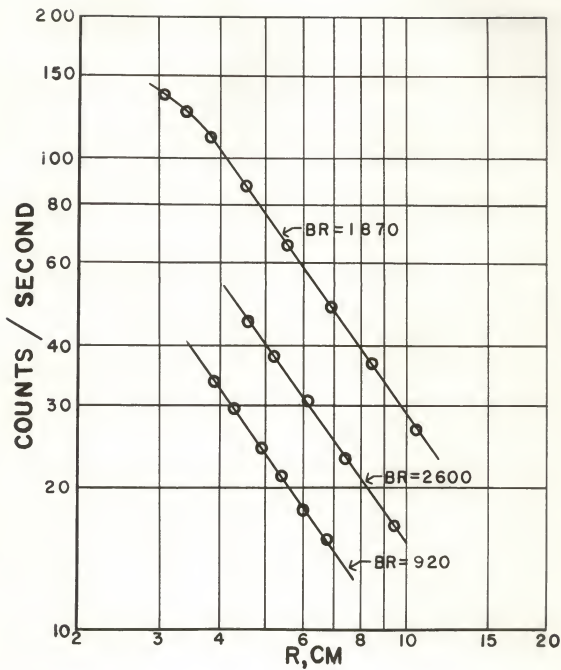
The  $\rho$ -factor was determined by examining a portion of the continuous beta spectrum, centered around a fixed  $B\rho$  value, taken at various radii. This was accomplished by observing the counting rates for a fixed spectral region at different magnetic field values of 555, 486, 408, 333, 267, 219, and 179 gaussess. To facilitate locating the spectral regions the strong K-conversion lines of the 316 kev and 468 kev gamma rays of iridium were first scanned. Then careful measurements of the continuous beta spectrum on both sides of these lines were taken. As shown on Plate III, a simple power law was adequate to account for the varying solid angle to within a percent or two, for radii down to the order of 4 centimeters. The behavior at smaller radii was sensitive to rather small changes in the geometric source configuration.

To ascertain if scattering from the camera walls would distort the spectrum, since the camera has no other baffling system than that of the source defining slits, temporary baffles were installed in the camera, allowing to pass only a small portion of the spectrum around 400 kev. Counting rates for the spectral region which should have been completely passed by the baffle system were found to be the same as those taken without the baffles, thus proving that scattering from the walls was not an important factor, at least above 400 kev. This data is summarized by the

EXPLANATION OF PLATE III

Variation of counting rates with focusing radius for  
three different values of BR. A power law exponent of  
 $1.38 \pm .01$  fits all curves down to 4 cm.

PLATE III





graph shown on Plate IV. Curve A shows the counting rates taken without the baffles, while curve B shows the counting rates taken with the baffles installed.

The backlash of the geiger tube was checked by rerunning the tube over the same conversion line. The consistency of the conversion line position showed that there was no appreciable backlash if precautions normal with spindle driven equipment were observed, such as approaching the conversion line from the same direction.

#### Discussion of Results

Along with other corrections inherent in all spectrometers, such as window transmission and dead time corrections, the  $\rho$ -factor furnishes the remaining information necessary to employ the variable radius spectrometer for quantitative intensity measurements.

The analysis of beta spectra was felt to be adequate to energies as low as 200 kev. For lower energies much greater care in source preparation would be necessary (Albert and Wu, 1). Beta spectrum end point determinations were good, since the fixed fields employed could be determined accurately, at leisure, by comparison with known standard energies.

The instrument performed very well in the study of weakly converted lines, particularly at high energies. There were no difficulties in field stabilisation, and further, a photographic plate taken previously served as a map for surveying such regions. Plate V shows the

EXPLANATION OF PLATE IV

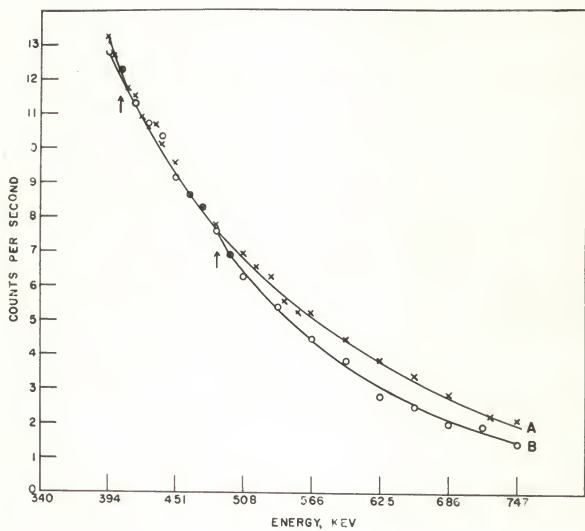
The Effects of Scattering from the Camera Wall

Curve A shows the counting rates taken without the baffles.

Curve B shows the counting rates taken with the baffles.

The energy region between the arrows represents the calculated zone for perfect transmission through the baffle aperture.

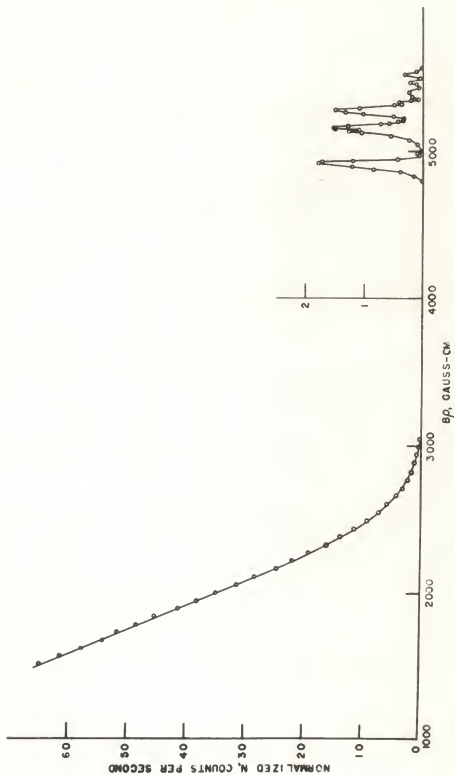
PLATE IV



EXPLANATION OF PLATE V

Shown here is the normalized beta spectrum of  $Ta^{182}$ . The normalized high energy conversion electron spectrum of  $W^{182}$  is also shown.

PLATE V



plot of the high energy conversion lines in  $W^{182}$ . Several of the conversion lines shown here are less intense than 1 part in 10,000 of the continuous beta spectrum.

#### INVESTIGATION OF $Ta^{182}$

$Ta^{182}$  decays by beta minus emission to excited  $W^{182}$ , which is a complex gamma-emitting nucleus of even-even species. Muller, et al. (18) has reported sixteen gamma rays and incorporated ten in partial decay schemes. One of the partial decay schemes and the remaining six gamma rays reported by Muller, as well as many other gamma rays found experimentally here have been incorporated into the energy level diagram shown in Plate VI.

#### Experimental Methods

Fixed field 180° focusing spectrometers were used to obtain conversion line energies. Since a large number of conversion lines were very weak in intensity, many photographic plates of varying exposures were required at each field setting. Short exposures were usually best for analysis of the low energy region while longer exposures were usually required for analysis of the high energy region. The magnetic fields were also varied so different regions could be studied more easily.

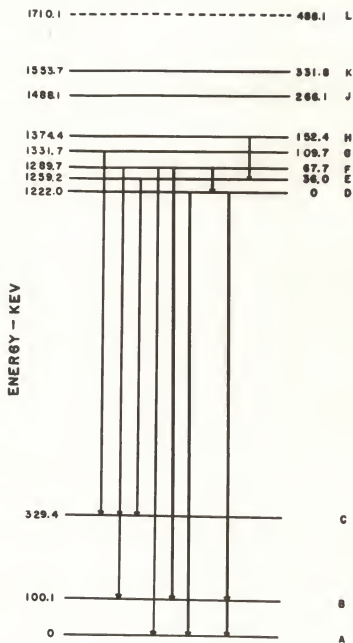
The lines on the plates were then measured carefully by several investigators to substantiate very weak lines. For the more intense line, comparator readings were taken, thus allowing accurate focusing

#### EXPLANATION OF PLATE VI

The energy level diagram of  $W^{182}$  is presented here.  
The designated energies to the right are for convenience when referring to the partial decay scheme proposed by Muller, et al.



## PLATE VI

 $W^{182}$ 

radii calculations. Accurate field values were determined by measurement of focusing radii for certain standard conversion groups. These standard groups have very precisely determined energies, and thus precisely known values of  $E\rho$  (18).

The analysis of the many plates taken showed well over one hundred conversion groups. Out of this large group of lines, the most intense, as well as several weaker but well substantiated lines, are listed in Table 1. The K-conversion lines are listed, as well as some relative intensities. Also listed are some direct gamma ray measurements and relative intensities as reported by Muller, et al. (18).

The intense high energy conversion lines, AD, EF, and ED were surveyed carefully using the variable radius spectrometer, so that their relative intensities were accurately determined. Even though the lines were classified as intense, the small solid angles subtended at radii of approximately 10 centimeters, reduced the line peak counting rates to only a few tenths of a count per second above background, thus making it necessary to reduce the background to a minimum. The background was composed of gamma radiation leakage from the source, cosmic radiation, and stray radiation within the laboratory. Lead blocks were placed around the camera to reduce the stray radiation. The gamma ray leakage from the source was reduced by placing 6 inches of lead absorber between the source and the geiger tube as shown in Plate I, Fig. 2. To measure the background a 1/2 inch piece of lucite was placed over the source defining slits to stop the conversion electrons. Background counting rates were then recorded at intervals over the spectral region to be surveyed.

Table 1. Energies of K-conversion lines with some of their relative intensities; also some gamma ray energies with relative intensities as reported by Muller, et al. (18).

Plate VI Designation	K-conversion Energy (keV)	Relative* Intensity	Y-ray Energy (keV)	Relative * Intensity
FH	15.2 ± 0.3		84.67 ± .01	6
AB	30.6 ± 0.5		100.09 ± .01	46
DG	40.3 ± 0.5			
HJ	44.1 ± 0.2		113.66 ± .01	9
EH	46.7 ± 0.5		116.40 ± .01	2
DH	82.1 ± 1.0		152.41 ± .02	43
KL			156.37 ± .02	14
HK	109.9 ± 1.0		179.36 ± .03	19
FJ	128.1 ± 1.0		198.30 ± .04	9
JL	152.6 ± 0.5		222.05 ± .04	45
GK	152.6 ± 0.5			
BC	159.5 ± 0.5		229.27 ± .05	24
FK	194.3 ± 1.0		264.09 ± .06	27
EK	226.7 ± 1.0			
AC	260.0 ± 1.0			
HL	265.7 ± 0.8			
CD	823.9 ± 1.3			
CE	860.0 ± 1.0			
CF	889.9 ± 1.8			
GG	932.0 ± 1.8			
CH	976.4 ± 1.0			
ED	1052.5 ± 0.5	10.0	1121.14 ± 1.02	352
CJ	1089.6 ± 0.4			
BE	1089.6 ± 0.4			
EF	1119.8 ± 1.8	8.0	1187.74 ± 1.70	157
AD	1152.5 ± 0.6	8.0	1223.25 ± 1.21	334
BG	1160.8 ± 1.2	0.9		
AE	1188.0 ± 2.0	0.5		
BH	1205.0 ± 1.0	0.2		
AF	1219.9 ± 2.0	1.0		
AG	1261.5 ± 2.0			
AH	1303.0 ± 2.0			
BK	1384.1 ± 1.1			
BL	1539.0 ± 1.5			

\* The intensities are relative to the two experiments, and can be compared only in ratios.

The lucite piece was then removed and the counting rates were recorded at much closer intervals. After the background was subtracted and the  $\rho$ -correction applied, the high energy spectral region appeared as shown on Plate V.

The beta spectrum was also surveyed with the variable radius spectrometer. The method was similar to that employed for the high energy spectral region except that less lead shielding had to be employed. Enough lead was removed so that the geiger tube could be moved into the 175 kev region. Although the background rates were fairly high the spectrum was obtained down to 175 kev. To insure better end point results, the lead was increased to about 5 centimeters. The reduced background was determined and the higher energy beta spectrum was again run. Combining the results of these two runs, the beta spectrum was determined fairly accurately from 175 kev to the end point of approximately 540 kev. The normalized spectrum is shown on Plate V.

Attempts to analyze the beta spectrum into its several components proved somewhat disappointing. A group of low intensity conversion lines so obscured the region near the end point that good measurement of the interior end points and relative intensities of the other beta spectra present could not be realized from a Fermi-Kurie plot.

#### Discussion of Results

The energy levels of  $W^{182}$  proposed are shown in Plate VI. The fol-

lowing discussion is presented in support of the assignments made on Plate VI.

The portion of the diagram from 1222 kev and up, with the exception of the level E, was one of several proposed by Muller, et al.(18). Of sixteen gamma rays cited, most of which were measured with high precision by the Dumond curved crystal spectrometer (18), ten were incorporated in this portion of the decay scheme. The remaining six gamma rays were placed between AB, BC, EH, AD, BD, and EF. These energy assignments were based upon measurements taken from the beta ray spectrographs. Gamma rays AD and BD were found to differ by  $99.9 \pm 0.5$  kev. The triad of lines to level C were also sufficiently intense for accurate measurement of energy differences and helped support the diagram. Finally, high energy transitions from nearly all of the levels D through K to A, B, and C, have been observed, and agree with the proposed scheme. Evidence for level L has been observed, although according to the various possibilities proposed by Muller either level G or L may be present, but not both. The data actually favors a level at G, perhaps one kev lower than that given.

Including a few additional weak low energy radiations between some of the levels D through L, it is seen that this decay scheme accommodates about forty gamma rays. However, at least this many more have been observed and roughly classified. For the most part, these radiations are very weak and are due, no doubt, to additional levels between C and D. Also there is little doubt that some radiations arise from levels higher than K (or L). The measurement of a single half-life of 115.5 days

over a period of five and one half cycles was indication that these weak gamma rays do not arise from contaminants.

The electron spectrum gave relative K-conversion of 10:8.0:8.0 for the three strong lines, AD, EF, and ED. These combined with the gamma ray intensity data of Muller, listed in Table 1, gave the ratios of K-conversion coefficients for the gamma rays as 1:1.8:0.85. Consistent with other decay schemes in this nuclide region, the spin and parity of the two lowest levels, A and B, were assigned as  $0^+$  and  $2^+$  respectively. With these assignments the first and third conversion coefficients were compatible with a  $1^-$  assignment for level D. This assignment also fixed the conversion coefficient for EF, which fit an E2 transition. A choice of  $4^+$  for the level F was consistent with the trend of the levels from D upward to follow an approximate algebraic relation. Allowing for two additional levels, not shown on Plate VI for lack of accuracy, of approximately 5 and 205 kev above D, the level energies above D become asymptotic to the expression  $E_L = 3.70(L)(L+1)$ . The correct energy values are shown at the right of Plate VI. The values of L are numbered consecutively from D, upward, starting with  $L = 1$  for the D level.

The levels A, B, and C agree well with the Bohr-Mottelson formulation (3), with level C taken as  $4^+$ . A further level at  $695 \pm 0.5$  kev which has been justified from conversion line data would fit the third excited state predicted by this formulation. It is interesting to note that the level D also fits, in energy, the fourth excited state predicted by the theory, but the predicted spin value of  $8^+$  is manifestly at variance with the  $1^-$  assignment suggested above.

## ACKNOWLEDGMENT

The author wishes to express his grateful appreciation to Dr. Clarence M. Fowler for his excellent advice, encouragement, and help extended by him throughout the course of this research and in the preparation of this manuscript; to Mr. H. W. Kruse and Mr. Vahe Keshishian for their cooperation in compiling the data needed in this research project; to Mr. D. A. Kittis and Professor Emeritus E. V. Floyd for their expert advice in mechanics; and to the Atomic Energy Commission for its sponsorship of the author's half-time Assistantship throughout most of this research.



## BIBLIOGRAPHY

- (1) Albert, R. D., and C. S. Wu.  
The beta-spectrum of  $S^{35}$ . *Phys. Rev.* 74, 847. 1948.
- (2) Beach, Louis A., Charles L. Peacock, and Roger C. Wilkinson.  
The radiation of tantalum<sup>182</sup>, rhenium<sup>186,188</sup>, and gold<sup>199</sup>.  
*Phys. Rev.* 76, 1585. 1949.
- (3) Bohr, Aage, and Ben R. Mottelson.  
Rotational states in even-even nuclei. *Phys. Rev.* 90, 717.  
1953.
- (4) Campbell, C. G., and J. Kyles.  
The variable-radius semicircular magnetic focusing  $\beta$ -ray  
spectrometer. *Proc. Phys. Soc. B* 66, 911. 1953.
- (5) Cork, J. M.  
Gamma-radiation from tantalum, iridium, and gold. *Phys. Rev.*  
72, 581. 1947.
- (6) Cork, J. M., et al.  
A reinterpretation of the electron spectra of radioactive  
ytterbium and tantalum. *Phys. Rev.* 78, 95. 1950.
- (7) Cork, J. M., et al.  
Gamma-rays from tantalum 182. *Phys. Rev.* 75, 1778. 1949.
- (8) Dumond, Jesse W. M., and E. Richard Cohen.  
Our knowledge of the atomic constants  $F$ ,  $N$ ,  $m$ , and  $h$  in 1947,  
and of other constants derivable therefrom. *Rev. Mod. Phys.*  
20, 82. 1948.
- (9) Dumond, J. W. M., et al.  
The decay of  $Ta^{183}$ . *Phys. Rev.* 92, 202. 1953.
- (10) Goddard, C. Harold, and C. Sharp Cook.  
On the photoelectron spectrum of  $Ta^{182}$ . *Phys. Rev.* 76,  
1419. 1949.
- (11) Halliday, David.  
Introductory nuclear physics. New York: John Wiley and Sons,  
1950.

- (12) Hill, R. D., E. L. Church, and J. W. Mihelich.  
The determination of gamma-ray energies from beta-ray spectroscopy and a table of critical x-ray absorption energies. *Rev. Sci. Instr.* 23, 523. 1952.
- (13) Jnanananda, Swami.  
The  $\beta$  - radiations of antimony<sup>124</sup>, tantalum<sup>182</sup>, tungsten<sup>185</sup>, and iridium<sup>192</sup>. *Phys. Rev.* 72, 112h. 1947.
- (14) Kruse, Herald Wesley.  
Analysis and application of source tilting in a magnetic focusing beta-ray spectrometer. Unpublished M. S. thesis, Kansas State College, Manhattan, Kansas, 1952.
- (15) Mandeville, C. E., and Morris V. Scherb.  
Radiations from tantalum (182), antimony (122), and indium (116). *Phys. Rev.* 73, 340. 1948.
- (16) Mellor, George Pearson.  
The design and construction of a beta-ray spectrometer. Unpublished M. S. thesis, Kansas State College, Manhattan, Kansas, 1953.
- (17) Mihelich, J. W.  
Successive neutron capture in Ta. *Phys. Rev.* 91, 427. 1953.
- (18) Muller, David E., et al.  
Precision measurements of nuclear  $\gamma$ -ray wavelengths of Ir<sup>192</sup>, Ta<sup>182</sup>, RaTh, En, W<sup>187</sup>, Cs<sup>137</sup>, Au<sup>198</sup>, and annihilation radiation. *Phys. Rev.* 80, 775. 1952.
- (19) O'Meara, F. E.  
Gamma-spectrum of Ta<sup>182</sup>. *Phys. Rev.* 79, 1032. 1950.
- (20) Rall, Waldo, and Roger G. Wilkinson.  
Gamma- and beta-ray energies of some radioactive isotopes as measured by a thin magnetic lens beta-ray spectrometer. *Phys. Rev.* 71, 321. 1947.
- (21) Wu, Chien-Shiung.  
Recent investigations of the shapes of  $\beta$ -ray spectra. *Rev. Mod. Phys.* 22, 386. 1950.

INVESTIGATION OF THE DISINTEGRATION OF TA<sup>182</sup>

by

ROBERT JOSEPH KLOTZ

A. B., Kansas State Teachers College, Emporia, 1952

---

AN ABSTRACT OF A THESIS

submitted in partial fulfillment of the

requirements for the degree

MASTER OF SCIENCE

Department of Physics

KANSAS STATE COLLEGE  
OF AGRICULTURE AND APPLIED SCIENCE

1954

Investigation of the decay of  $Ta^{182}$  was carried out employing primarily,  $180^\circ$  focusing fixed field beta ray spectrometers.

Energy assignments as well as some spin assignments have been given for  $W^{182}$ . The basis for these assignments arose largely from the quantitative electron energy and intensity measurements made with the beta ray spectrometers. Lower energy levels followed the Bohr-Mottelson theory in both energy and spin assignments. Higher energy levels, measured from a 1222 kev level, became asymptotic to the expression:  $E_L = 3.70(L)(L+1)$ . Some of the spin assignments given for the spin values were consistent with the above expression.

Characteristics of the variable radius spectrometer were investigated so that quantitative intensity studies of the electron spectra could be realized. The changing solid angle subtended by the detector slit in the variable radius spectrometer was found to change by a simple radius power law, down to radii of the order of 4 cm. Other tests showed that scattering from the walls of the camera had no effect on the spectrum, above 400 kev.

Descriptions of the various instruments used were presented.